Electro-Mechanical Impedance Method for Crack Detection in Thin Plates

Andrei N. Zagrai and Victor Giurgiutiu*

University of South Carolina, Department of Mechanical Engineering, Columbia, SC 29208
*803-777-0619, Fax 803-777-8018, email victorg@sc.edu*

ABSTRACT: This paper describes the utilization of Electro-Mechanical (E/M) impedance method for structural health monitoring of thin plates. The method allows the direct identification of structural dynamics by obtaining its E/M impedance or admittance signatures. The analytical model for two-dimensions structure was developed and verified with experiments. Good matching of experimental results and calculated spectra was obtained for axial and flexural components. The ability of the method to identify the presence of damage was investigated by performing an experiment where the damage in the form of crack was simulated with An EDM slit placed at various distances from the sensor. It was found that the crack presence dramatically modifies the E/M impedance spectrum and this modification decreases as the distance between the sensor and the crack increases. Several overall–statistics damage metrics, which may be used for on-line structural heath monitoring, were investigated. Among these candidate damage metrics, the α-th power of the correlation coefficient deviation, CCD^α, $3 < \alpha < 7$, used in the high frequency band 300-450 kHz, was found to be most successful. Careful selection of the high frequency band and proper choice of the appropriate damage metric were found to be essential for successful damage detection and structural health monitoring.

INTRODUCTION

In recent years, the damage detection with E/M impedance method has gained increased attention. The method uses small-size piezoelectric active sensors intimately bonded to an existing structure, or embedded into a new composite construction. Experimental demonstrations have shown that the real part of the high-frequency impedance spectrum is directly affected by the presence of damage or defects in the monitored structure (Figure 1).

Pioneering work on utilization of E/M impedance method was presented by Liang *et al.* (1994) who performed the coupled E/M analysis of adaptive systems driven by a surface-attached piezoelectric wafer. However, no modeling of the structural substrate was included, and no prediction of structural impedance for a multi-DOF structure was presented. This work was continued and extended by Sun *et al.* (1994, 1995) who used the half-power bandwidth method to accurately determine the natural frequency values. While the structural dynamics was always accounted for in the solution, the majority of authors assumed that the stiffness of the piezoelectric sensor is static and no sensor dynamics was considered. Giurgiutiu and Zagrai (2001a) derived an expression where the dynamics of a sensor was incorporated and the E/M impedance spectrum was modeled to simulate the direct measurements at the sensor's terminals.

*Author to whom correspondence should be addressed
E-mail: victorg@sc.edu

The authors limited themselves to the one-dimension structure. Thus, the modeling was verified with simple beam specimen. In the same reference, the method for sensor's self-diagnostics was suggested.
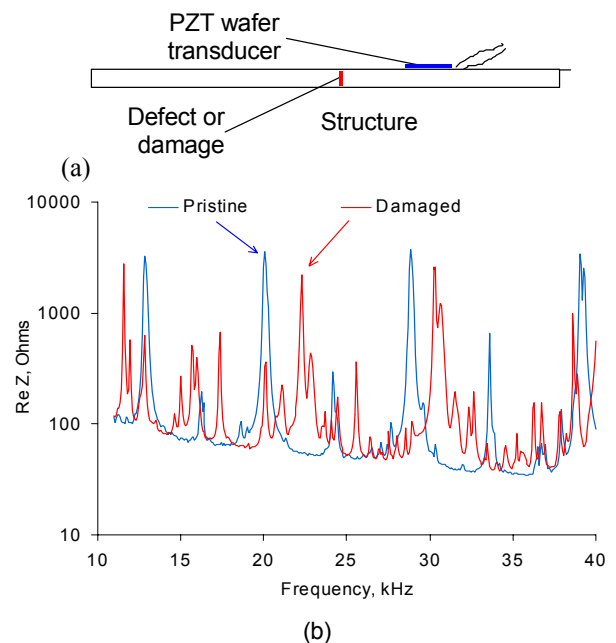
Figure 1. PZT wafer transducer acting as active sensor to monitor structural damage: (a) mounting of the PZT wafer transducer on a damaged structure; (b) the change in E/M impedance due to the presence of a crack.

The experimental efforts to utilize the E/M impedance method for complex structures were highly investigated. The application of the method has been proven in various engineering fields, such as: aerospace structures (Chaudhry *et al*, 1994, 1995; Giurgiutiu and Zagrai, 2000; Giurgiutiu *et al.,* 2001), bolted joints (Estaban *et al*., 1996;), spot-welded joints (Giurgiutiu *et al.*, 2000); civil structures (Ayres, *et al*, 1996; Park et al., 2000b; Tseng *et al.*, 2000), spur gears (Childs *et al*., 1996), pipeline systems (Park et al., 2001). The method has been shown to be especially effective at ultrasonic frequencies, which properly capture the changes in local dynamics due to incipient structural damage. (Such changes are too small to affect the global dynamics and hence cannot be readily detected by conventional low-frequency vibration methods). Novel ways to interpret the high-frequency impedance spectra generated by this technique, and to identify the changes due to the presence of structural damage have been explored by Lopez et *al.* (2000) Park et al. (2000a), Tseng *et al.* (2001), and Monaco *et al.* (2001).

In this paper, the theoretical analysis for 2-D isotropic circular plates structures is presented. Both, axial and flexural components of natural vibrations are included for in the solution. Theoretical analysis is performed for particular boundary conditions to model the experimental set-up. The analytical model is validated with experimental results. Systematic experiments conducted on statistical samples of incrementally damaged specimens were used to fully understand and calibrate the investigative method. Good matching between theoretical prediction and experimental data is illustrated.

MODELING OF A PZT ACTIVE SENSOR INSTALLED ON A STRUCTURAL SUBSTRATE

The goal of this analysis is to develop a model for E/M impedance spectrum as measured at the sensors terminals, and account for the geometry and boundary conditions presented by the host structure onto the sensor. The dynamics of the sensor will be obtained by solving the problem of axial vibration of a piezoelectric disk with stiffness boundary condition represented by the pointwise dynamic structural stiffness $k_{str}(\omega)$. The dynamics of a host structure is described by poitwise dynamic structural stiffness $k_{str}(\omega)$. The dynamic structural stiffness accounts for both axial and flexural vibrations of the host structure. This means that $k_{str}(\omega)$ is defined by considering both axial and flexural vibrations of circular plates under steady state excitation produced by piezoelectric active sensor.

THE PZT ACTIVE SENSOR IMPEDANCE

The linear constitutive equations for piezoelectric materials in cylindrical coordinates are (Onoe *et al.*, 1967; Pugachev, 1984; IEEE Std 176, 1987):

$$S_{rr} = s_{11}^E T_{rr} + s_{12}^E T_{\theta\theta} + d_{31} E_z$$
$$S_{\theta\theta} = s_{12}^E T_{rr} + s_{11}^E T_{\theta\theta} + d_{31} E_z \ , \tag{1}$$
$$D_z = d_{31}\left(T_{rr} + T_{\theta\theta}\right) + \varepsilon_{33}^T E_z$$

Using the strain-displacement relationships for axis-symmetric motion,

$$S_{rr} = \frac{\partial u_r}{\partial r}, \ S_{\theta\theta} = \frac{u_r}{r},$$

where u_r is the radial displacement, yield stresses in terms of displacement and applied electric field:

$$T_{rr} = \frac{1}{s_{11}^E\left(1-v^2\right)}\left(\frac{\partial u_r}{\partial r} + v\frac{u_r}{r}\right) - \frac{d_{31}E_z}{s_{11}^E\left(1-v\right)} \tag{2}$$

$$T_{\theta\theta} = \frac{1}{s_{11}^E\left(1-v^2\right)}\left(v\frac{\partial u_r}{\partial r} + \frac{u_r}{r}\right) - \frac{d_{31}E_z}{s_{11}^E\left(1-v\right)} \tag{3}$$

Applying Newton's second law of motion at infinitesimal level yields

$$\frac{\partial T_{rr}}{\partial r} + \frac{T_{rr} - T_{\theta\theta}}{r} = \rho \cdot \frac{\partial^2 u_r}{\partial t^2} \tag{4}$$

Upon substitution, one recovers the equation of motion in cylindrical coordinates:

$$\frac{\partial^2 u_r}{\partial r^2} + \frac{1}{r}\frac{\partial u_r}{\partial r} - \frac{u_r}{r^2} - \frac{1}{c}\frac{\partial^2 u_r}{\partial t^2} = 0 \tag{5}$$

where $c = 1/\sqrt{\rho s_{11}^E \cdot (1-v_a^2)}$ is the sound speed in PZT disk for axially symmetric radial motion. Note that the equation of motion (4) does not contain the piezoelectric effect, d_{31}, E_3 explicitly. However, the piezoelectric effect appears explicitly in the terms of the T_{rr} and $T_{\theta\theta}$ stress equations (2) and (3), respectively. The general solution of Equation (5) is expressed in terms of the Bessel functions of the first kind, J_1, in the form

$$u_r(r,t) = A \cdot J_1\left(\frac{\omega r}{c}\right) e^{i\omega t} \tag{6}$$

The coefficient A is determined from the boundary conditions. Although the specialized literature presents the solution for the case of a free boundary condition at the circumference (Pugachev, 1984), no solution could be found for the case where the circumferential boundary condition is represented by an elastic constraint of known stiffness, $k_{str}(\omega)$. Hence, we developed, from the first principles, the solution for the electromechanical axial vibrations of a piezoelectric disk with elastic constraint of stiffness $k_{str}(\omega)$ around its circumference.
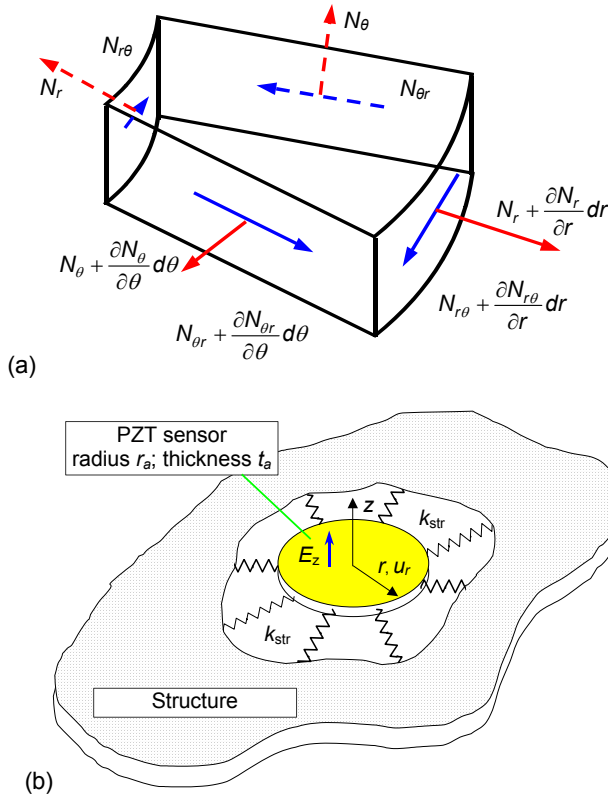
Figure 2. Analysis of axial axis-symmetric vibrations of a piezoelectric active sensor: (a) modeling set up; (b) PZT wafer active sensor constrained by structural stiffness, $k_{str}(\omega)$.

According to Figure 2, at the boundary $r = r_a$,

$$N_a(r_a) = -k_{str} \cdot u_r(r_a)$$

The radial and tangential stress components of piezoelectric disk are:

$$
\begin{aligned}
T_{rr}(r_a) &= \frac{N_a(r_a)}{t_a} = \frac{k_{str} u_{PZT}(r_a)}{t_a} \\
T_{\theta\theta}(r_a) &= \frac{1}{s_{11}^E}\left(\frac{u_r(r_a)}{r_a} - s_{12}^E T_{rr} - d_{31} E_z \right)
\end{aligned}
\tag{7}
$$

where N_a is a line force.

Using the constitutive equations for piezoelectric disk in terms of displacement and Equations (7) we obtain(Zagrai and Giurgiutiu, 2001):

$$
\begin{aligned}
\frac{\partial u_r(r_a)}{\partial r} &= s_{11}^E \frac{k_{str} u_r(r_a)}{t_a} \\
&+ \frac{s_{12}^E}{s_{11}^E}\left(\frac{u_r(r_a)}{r_a} - s_{12}^E \frac{k_{str} u_r(r_a)}{t_a} - d_{31} E_z \right) + d_{31} E_z
\end{aligned}
\tag{8}
$$

Denoting the static stiffness of the piezoelectric disk by $k_{PZT} = t_a / \left[r_a s_{11}^E (1-\nu) \right]$, and the dynamic stiffness ratio $\chi(\omega) = k_{str}(\omega)/k_{PZT}$ (Giurgiutiu and Zagrai 2001b), the above expression can be rearranged in the convenient form:

$$\frac{\partial u_r(r_a)}{\partial r} = \chi(\omega)\cdot(1+\nu)\frac{u_r(r_a)}{r_a} - \nu \frac{u_r(r_a)}{r_a} + (1+\nu)d_{31}E_z \tag{9}$$

where $\nu = -s_{12}^E / s_{11}^E$ is the Poisson ratio. Substituting $u_r(r_a)$ by the general solution for displacement given by Equation (6) allows us to find the constant A in the form:

$$A = \frac{(1+\nu)\cdot d_{31}E_0}{\frac{\omega}{c}J_0\left(\frac{\omega r_a}{c}\right) - \frac{\left(1-\nu+\chi(\omega)\cdot(1+\nu)\right)}{r_a}\cdot J_1\left(\frac{\omega r_a}{c}\right)} \tag{10}$$

Using the constitutive equations of piezoelectric disk (1) yields the electric displacement D_z as:

$$D_z = \left(\frac{d_{31}(1+\nu)}{s_{11}^E(1-\nu^2)}\frac{\omega}{c}AJ_0\left(\frac{\omega r}{c}\right) - \left(\frac{2d_{31}^2}{s_{11}^E(1-\nu)} + \varepsilon_{33}^T\right)E_0 \right)e^{i\omega t} \tag{11}$$

Integration of Equation (11) yields the charge:

$$
\begin{aligned}
Q &= \int_0^{2\pi} d\theta \int_0^{r_a} D_z r dr = \pi r_a^2 \varepsilon_{33}^T E_0 e^{i\omega t} \\
&\times \left[1 - k_p^2 + k_p^2 \frac{(1+\nu)J_1(\varphi_a)}{\varphi_a J_0(\varphi_a) - (1-\nu+\chi(\omega)\cdot(1+\nu))\cdot J_1(\varphi_a)} \right]
\end{aligned}
\tag{12}
$$

where $\varphi_a = \omega r_a / c$, while r_a is the radius of a disk, and $k_p = \sqrt{2d_{31}^2 / \left[s_{11}^E \cdot (1-\nu_a)\varepsilon_{33}^T \right]}$ is the planar coupling factor.

The electrical admittance in terms of harmonic electrical current and voltage is $Y = \hat{I}/\hat{V}$. Since $\hat{I} = i\omega \cdot \hat{Q}$ and $\hat{E} = \hat{V}/t_a$, Equation (12) yields the admittance expression for piezoelectric disk sensor constrained by the structural substrate with dynamic stiffness ratio $\chi(\omega)$:

$$
\begin{aligned}
Y(\omega) &= i\omega C\left(1-k_p^2\right) \\
&\times \left[1 + \frac{k_p^2}{1-k_p^2}\frac{(1+\nu)J_1(\varphi_a)}{\varphi_a J_0(\varphi) - (1-\nu)J_1(\varphi_a) - \chi(\omega)(1+\nu)J_1(\varphi_a)} \right]
\end{aligned}
\tag{13}
$$

The sensor impedance, $Z(\omega)$, can be found using the relationship

$$
\begin{aligned}
Z(\omega) &= \frac{1}{i\omega C\left(1-k_p^2\right)} \times \\
&\left\{ \left[1 + \frac{k_p^2}{1-k_p^2}\frac{(1+\nu)J_1(\varphi_a)}{\varphi_a J_0(\varphi) - (1-\nu)J_1(\varphi_a) - \chi(\omega)(1+\nu)J_1(\varphi_a)} \right] \right\}^{-1}
\end{aligned}
\tag{14}
$$

Equation (14) can be used to predict the E/M impedance spectrum as it would be measured by the impedance analyzer at the embedded active-sensor terminals during a

structural heath monitoring process. Thus, it allows for direct comparison between experimental spectrum measured with the impedance analyzer and the spectrum predicted by Equation (14).

MODELING OF A CIRCULAR PLATE SUBSTRATE

The theoretical foundation for transverse vibrations of isotropic circular plates was first published by Airey (1911) and extended by Colwell (1936). An outstanding overview of a subject was presented by Leissa (1969). The theoretical background and numerical results were given for large variety of boundary conditions and plate shapes. (Wah, 1962; Kunukkasseril and Swamidas, 1974; Soedel, 1993; Rao, 1999). The equation of motion for axis-symmetric axial and flexural vibration of circular plates is:

$$\frac{Eh}{1-v^2}\left(\frac{\partial^2 u_r}{\partial r^2}+\frac{1}{r}\frac{\partial u_r}{\partial r}-\frac{u_r}{r^2}\right)-\rho h \cdot \frac{\partial^2 u_r}{\partial t^2}=-\left(\frac{\partial N_r^e}{\partial r}+\frac{N_r^e}{r}\right) \quad (15)$$

$$D\nabla^4 w+\rho h \cdot \frac{\partial^2 w}{\partial t^2}=\frac{\partial^2 M_r^e}{\partial r^2}+\frac{2}{r}\frac{\partial M_r^e}{\partial r} \quad (16)$$

where u_r is the radial in-plane displacement, and w is the transverse displacement.

Consider the piezoelectric disk sensor placed at the origin of the plate as it is shown in the Figure 3. For further consideration, it is convenient to formulate our problem in terms of total displacement of piezoelectric sensor bonded at the origin of the circular plate undergoing axial and flexural vibrations. When the sensor is excited with an external voltage, it elongates due to piezoelectric effect and produces a force F_a which induces a force and moment on the plate (Figure 4). When the excitation is harmonic with circular frequency ω, the line force and line moment produced by PZT are:

$$N_r^e(r,t)=N_r^a(r) \cdot e^{i\omega t} \quad (17)$$

$$M_r^e(r,t)=M_r^a(r) \cdot e^{i\omega t} \quad (18)$$

Due to the problem's axial symmetry, the θ-dependent component is not present in the solution. The magnitude of the excitation line force and line moment of Equations (17), (18) is defined in terms of the Heaviside function:

$$N_r^a(r)=N_a \cdot \left[H(r_a-r)\right] \qquad M_r^a(r)=M_a \cdot \left[H(r_a-r)\right]$$
$$(r \in [0,\infty)) \quad (19)$$
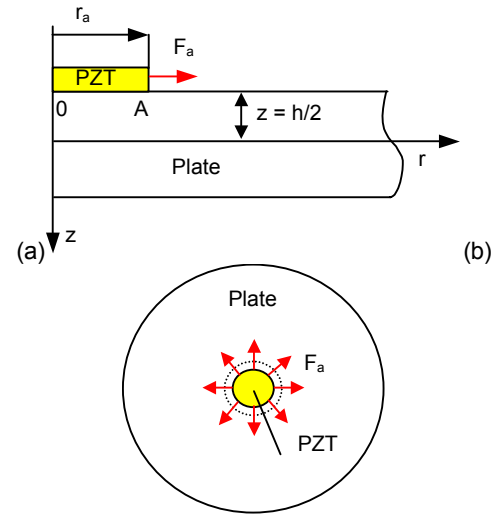
Figure 3. Schematics on elongation of piezoelectric sensor bounded on the plate: (a) side view; (b) top view.
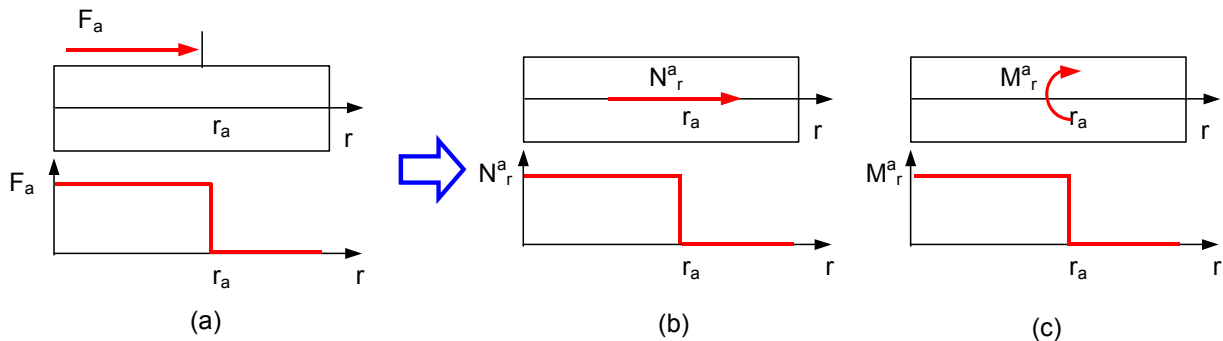
Figure 4. Schematic of the excitation induced by a circular piezoelectric sensor on a circular plate: (a) force F_a from active sensor becomes, (b) axial force, N_r^a, plus (c) moment, M_r^a

The solution of Equations (15) and (16) is expressed as series expansions in terms of modeshape functions:

$$u_r(r,t) = \left(\sum_k P_k R_k(r) \right) \cdot e^{i\omega t},$$

$$\frac{E}{\rho \cdot (1-v^2)} \left(R_k''(r) + \frac{1}{r} R_k'(r) - \frac{1}{r^2} R_k(r) \right) = -\omega_k^2 \cdot R_k(r) \quad (20)$$

$$w(r,t) = \left[\sum_m G_m \cdot Y_m(r) \right] \cdot e^{i\omega t}, \ D \cdot \nabla^4 Y_m(r) = \omega_m^2 \cdot \rho h \cdot Y_m(r) \quad (21)$$

where ω_k and ω_m correspond to the natural frequencies of axial and flexural vibrations with corresponding modal participation factors P_k and G_m. The solutions for modeshapes R_k and Y_m for axial and flexural vibrations of circular plate are expressed in terms of Bessel functions for particular boundary conditions (Itao and Crandall, 1979):

$$R_k(r) = A_k J_1(\lambda_k r) \quad (22)$$

$$Y_m(r) = A_m \cdot \left[J_0(\lambda_m r) + C_m \cdot I_0(\lambda_m r) \right] \quad (23)$$

The modeshapes R_k and Y_m of Equations (22), (23) form ortho-normal sets of functions defined by the following conditions:

$$\rho h \cdot \int_0^a \int_0^{2\pi} R_k(r) R_l(r) r dr d\theta$$
$$= \rho h \cdot \pi a^2 \cdot \delta_{kl} = \rho h \cdot \pi a^2 \cdot \begin{cases} 1 & k = l \\ 0 & k \neq l \end{cases} \quad (24)$$

$$\rho h \cdot \int_0^a \int_0^{2\pi} Y_p(r) \cdot Y_m(r) r dr d\theta = m \cdot \delta_{pm} = \pi a^2 \cdot \rho h \cdot \delta_{pm} \quad (25)$$

where a is a radius of a circular plate, h is the thickness, and ρ is the density.

Using expressions Equations (15)-(25), the modal participation factors for axial and flexural vibrations obtained as:

$$P_k = \frac{2N_a}{\rho h \cdot a^2} \cdot \frac{\left[r_a R_k(r_a) + \int_0^a R_k(r) \cdot H(r_a - r) dr \right]}{\left(\omega_k^2 - 2i\varsigma_k + \omega^2 \right)} \quad (26)$$

$$G_m = \frac{2M_a}{\rho h \cdot a^2} \frac{\left[Y_m(r_a) - r_a \cdot Y_m'(r_a) \right]}{\left(\omega_m^2 - 2i\varsigma_m + \omega^2 \right)} \quad (27)$$

where ζ_k and ζ_{mn} are the modal damping ratios.

DYNAMIC STRUCTURAL STIFFNESS

The radial displacement of piezoelectric sensor consists of axial and flexural parts:

$$u_{PZT}(r_a, t) = u_{PZT}^{Axial}(r_a, t) + u_{PZT}^{Flexural}(r_a, t)$$

and is described by

$$u_{PZT}(r_a, t) = u_0(r_a, t) - \frac{h}{2} \cdot w'(r_a, t)$$

where $w(r_a, t)$ is the bending displacements of the neutral axis. Referring to the Figure 3, the difference between points A and 0 yields

$$u_{PZT}(r_a, t) = u_A(r_a, t) - u_0(0, t)$$
$$= \sum_k P_k R_k(r_a) \cdot e^{i\omega t} - \frac{h}{2} \sum_m G_m Y_m'(r_a) \cdot e^{i\omega t} \quad (28)$$

Substitution Equations (26) and (27) into Equation (28) gives the following result for the axial displacement of piezoelectric active sensor:

$$\hat{u}_{PZT} = \frac{N_a}{a^2 \cdot \rho} \left[\frac{2}{h} \cdot \sum_k \frac{\left[r_a R_k(r_a) + \int_0^a R_k(r) \cdot H(r_a - r) dr \right] R_k(r_a)}{\left(\omega_k^2 - 2i\varsigma_k + \omega^2 \right)} \right]$$
$$+ \frac{N_a}{a^2 \cdot \rho} \left[\frac{h}{2} \cdot \sum_m \frac{\left[Y_m(r_a) - r_a \cdot Y_m'(r_a) \right] \cdot Y_m'(r_a)}{\left(\omega_m^2 - 2i\varsigma_m + \omega^2 \right)} \right] \quad (29)$$

The dynamic structural stiffness can defined in terms of the line force N_a and the displacement of piezoelectric active sensor. Defining the structural stiffness, k_{str}, as:

$$k_{str} = \frac{N_a}{\hat{u}_{PZT}} \quad (30)$$

Equation (29) yields the total dynamic structural stiffness:

$$k_{str}(\omega) = a^2 \rho$$
$$\times \left[\cdot \frac{2}{h} \cdot \sum_k \frac{\left[r_a R_k(r_a) + \int_0^a R_k(r) \cdot H(r_a - r) dr \right] R_k(r_a)}{\left(\omega_k^2 - 2i\varsigma_k + \omega^2 \right)} \right.$$
$$\left. + \frac{h}{2} \cdot \sum_m \frac{\left[Y_m(r_a) - r_a \cdot Y_m'(r_a) \right] \cdot Y_m'(r_a)}{\left(\omega_m^2 - 2i\varsigma_m + \omega^2 \right)} \right]^{-1} \quad (31)$$

MODEL VALIDATION THROUGH NUMERICAL AND EXPERIMENTAL RESULTS

A series of experiments were conducted on thin-gage aluminum plates to validate the theoretical investigation. Twenty five identical circular plates were manufactured from aircraft-grade aluminum stock. The diameter of each plate was 100-mm and the thickness was approximately 0.8-mm. The plates were instrumented with 7-mm diameter piezoelectric-disk active sensor, placed at the plate center (Figure 5a). The twenty five plates were split into five "pristine" plates and twenty "damaged" plates.

Impedance data was taken using a HP 4194A Impedance Analyzer. The spectra reordered during this process are shown in Figure 5b. During the experiments on five "pristine" plates (Group 0), the specimens were supported

on commercially available packing foam to simulate free boundary conditions. Plate resonance frequencies were identified from the E/M impedance real part spectra. Table 1 shows the statistical data in terms of resonance frequencies and log_{10} amplitudes. It should be noted that the resonance frequencies have very little variation (1% standard deviation) while the log_{10} amplitudes vary more widely (1.2—3.6% standard deviation).

In Figure 6, the experimental spectrum was compared with the spectrum predicted by to the theory presented in this paper. The modified expression (14) was used to simulate E/M impedance spectrum for a particular plate used in the preceding experiment. Figure 6a shows this comparison over wide frequency range (0.5 - 40 kHz), which captures six flexural and one axial modes. Figure 6b zooms into the 0.5 – 8 kHz range, and identifies the first three flexural modes of the circular plate. The theoretical predictions of Figure 6 were obtained with modified version of Equation (14). The modifications consisted in introducing a multiplicative correction factor a/r_a, in front of the stiffness ratio $\chi(\omega)$.

Although the simulation gives a good matching with experimental results, the model is limited to the natural frequencies corresponding to the purely axis-symmetrical modes. This assumption is consistent with the geometry of our problem where the piezoelectric disk active sensor was placed in the center of the plate. However, if the sensor is slightly misaligned non axis-symmetric modes will also be excited and appear in the spectrum. This effect is especially noticeable at high frequencies as illustrated in Figure 6a. Low amplitude peaks that appeared due to slight misalignment of the sensor from the plate center are observable at 15, 24 and 33 kHz

DAMAGE DETECTION EXPERIMENTS

Systematic experiments were performed to assess the detection of cracks. The experimental setup is shown in Figure 7. Five groups were considered: one group consisted of pristine circular plates (Group 0) and four groups consisted of plates with simulated cracks placed at increasing distance from the plate edge (Group 1 through 4). In our study, a 10-mm circumferential EDM (electric discharge machining) slit was used to simulate an in-service crack. During the experiments, the specimens were supported on packing foam to simulate free conditions.

Table 1. Statistical summary for resonance peaks of first four axis-symmetric modes of a circular plate as measured with the piezoelectric active sensor using the E/M impedance method.

Statistical Summary for Group 0 -- Pristine			
Average frequency, kHz	Frequency STD, kHz (%)	Log_{10} - Average amplitude, Log_{10} - Ohms	Log_{10} - Amplitude STD, Log_{10} - Ohms (%)
12.856	0.121 (1%)	3.680	0.069 (1.8%)
20.106	0.209 (1%)	3.650	0.046 (1.2%)
28.908	0.303 (1%)	3.615	0.064 (1.7%)
39.246	0.415 (1%)	3.651	0.132 (3.6%)

(a)   (b)
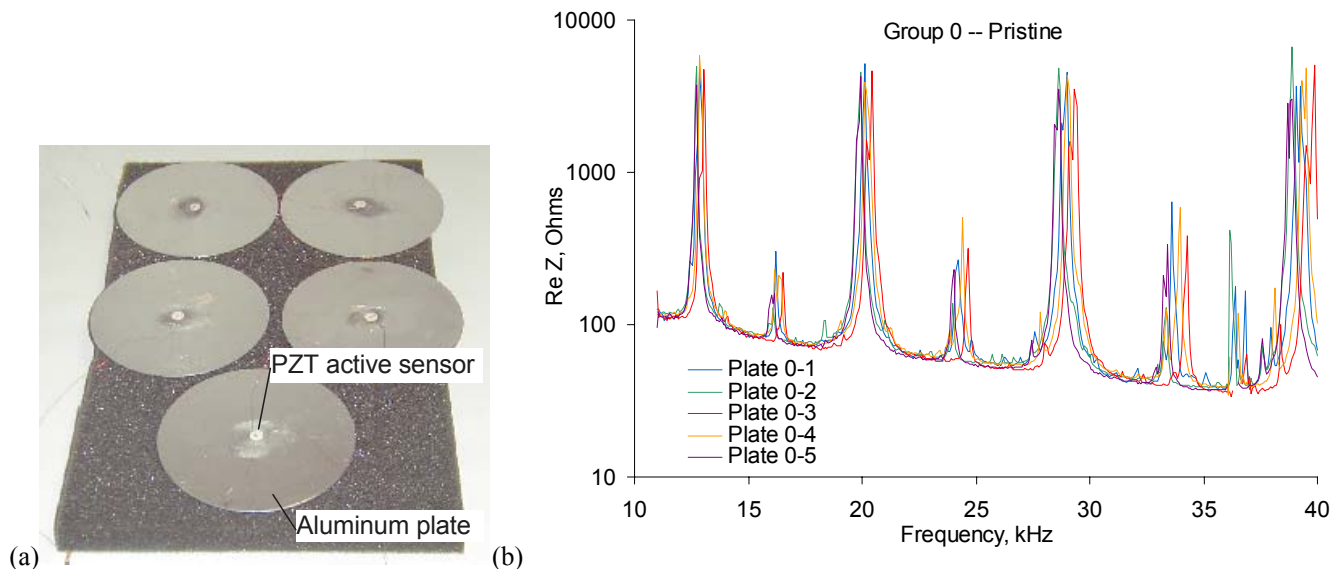
Figure 5. (a) Thin-gage aluminum plate specimens with centrally located piezoelectric sensors: 100-mm circular plates, thickness – 0.8mm. (b) E/M impedance spectra taken from pristine plates in the 11—40 kHz frequency band.

The experiments were conducted over three frequency bands: 10-40 kHz; 10-150 kHz, and 300-450 kHz. The data was process by capturing the real part of the E/M impedance spectrum, and determining a damage metric to quantify the difference between two spectra. Figure 8 shows data in the 10-40 kHz band. The superposed spectra of groups 0 and 4 specimens (extreme situations) are shown in Figure 8a, while those of groups 0 and 1 (almost similar situations) are shown in Figure 8b. Figure 8a indicates that the presence of the crack in the close proximity of the sensor drastically modifies the real part of the E/M impedance spectrum. Resonant frequency shifts and the appearance of new resonances are noticed. In contrast, the presence of the crack in the far field only marginally modifies the frequency spectrum (Figure 8b).
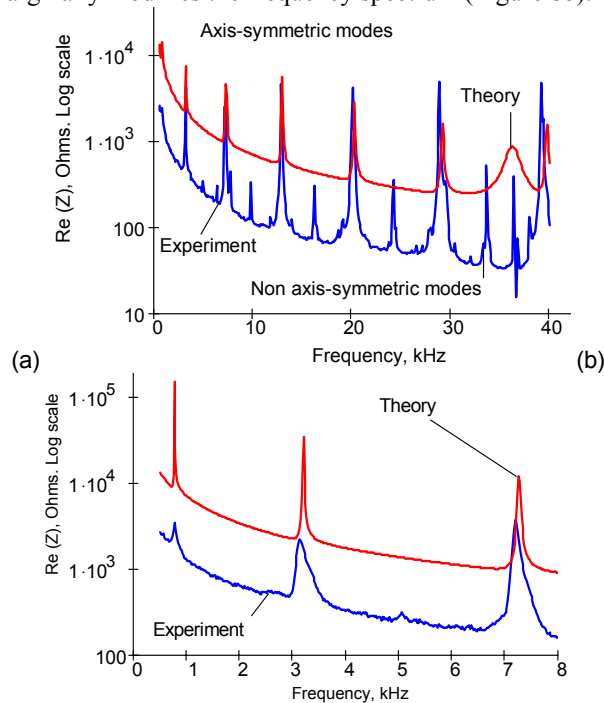

Figure 6. Experimental and calculated E/M impedance spectra for pristine plate specimen: (a) 0.5-40 kHz frequency range; (b) 0.5-8 kHz frequency range.

For the high frequency band, similar results were obtained. Figure 9a shows the extreme situation where the spectrum of the pristine plate (Group 0) was compared with the spectrum of a plate having the crack placed in the proximity of the sensor (Group 4). Significant difference between the two spectra is noticeable. When the crack was in the far field (Group 1), the sensor was also able to capture the presence of the damage but the changes in the spectrum were less severe (Figure 9b). Thus, the results obtained in the high frequency band follow the trend already observed in the lower frequency band.

Development of suitable damage metrics and damage identification algorithms remain an open question in the practical application of E/M impedance technique. The damage index is a scalar quantity that serves as a metric for the damage present in the structure. The damage index compares the amplitudes of the two spectra (damaged vs. pristine) and assigns a scalar value. Ideally, the damage index should be able to evaluate the E/M impedance spectrum and indicate damage presence, location, and severity. Sun *et al.* (1995) used a damage index based on the root mean square deviation (RMSD) of the E/M impedance real part spectrum. Though simple and extensively used, the RMSD metric has an inherent problem: perturbing effects unrelated to damage (e.g., temperature variation) shift up and down the spectrum, and directly affect the damage index value. Compensation of such effects is not straightforward, and may not even be possible. Other damage metrics, based on alternative statistical formulae (absolute percentage deviation, the covariance, the correlation coefficient, etc.) have also been tried (Tseng *et al.* 2001; Monaco *et al.*, 2001). However, this did not seam to completely alleviate this problem.

In our experimental study, we used several overall-statistics damage metrics to quantify the difference between spectra for various crack locations: root mean square deviation (RMSD); mean absolute percentage deviation (MAPD); covariance change (CC); correlation coefficient deviation (CCD). We found the correlation coefficient deviation to be the best metric of damage presence.
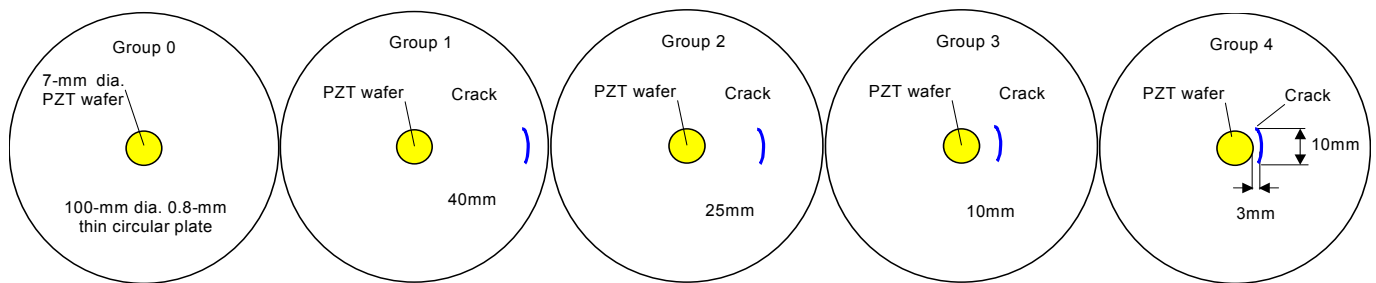
Figure 7. Systematic study of circular plates with simulated cracks (EDM slits) placed at decreasing distance from the E/M impedance sensor.
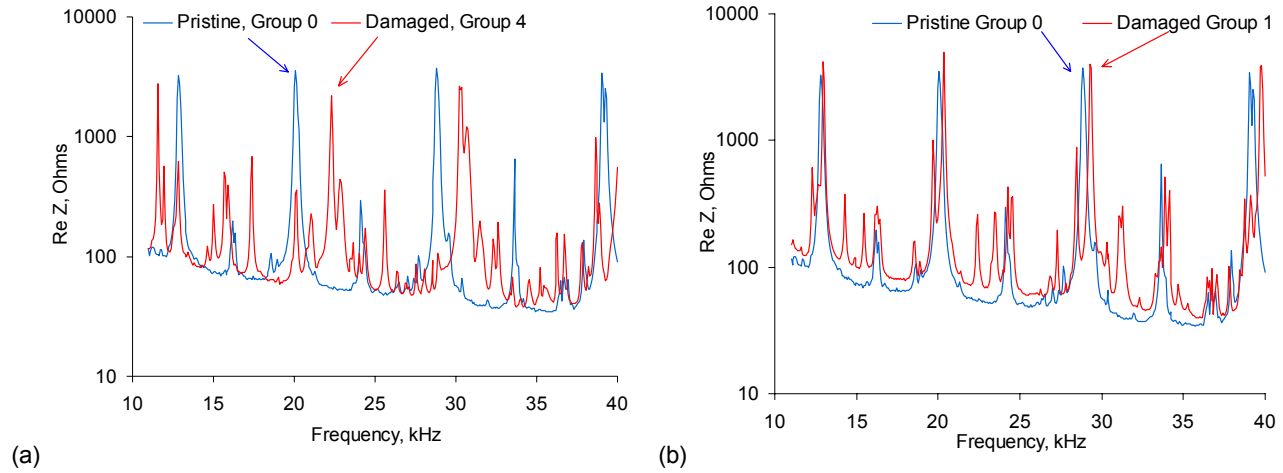
Figure 8. E/M impedance results in the 10—40 kHz band: (a) superposed groups 0 & 4 spectra; (b) superposed groups 0 & 1 spectra.
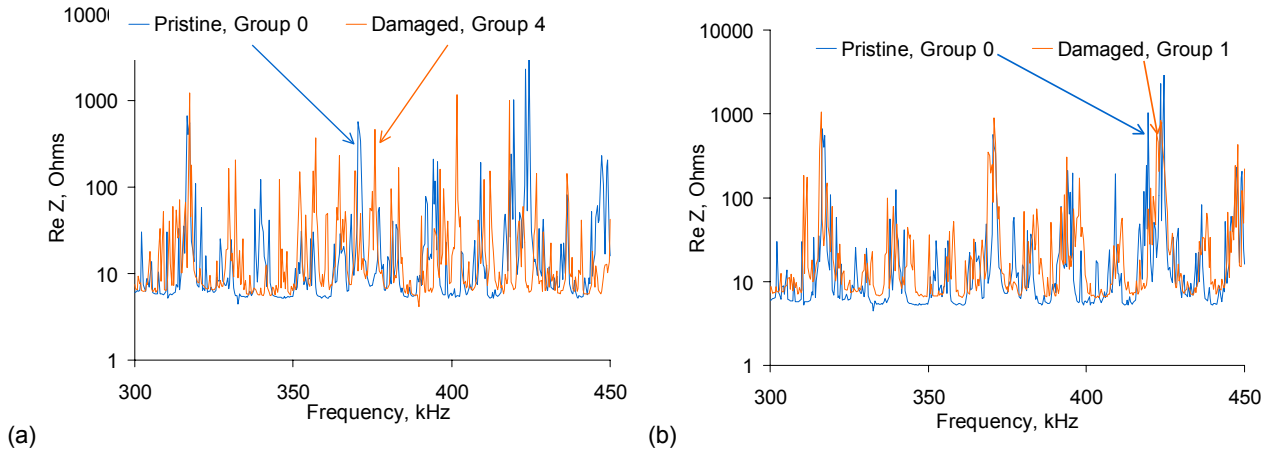
Figure 9. E/M impedance results in the 300–450 kHz band: (a) superposed Groups 0 & 4 spectra; (b) superposed Groups 0 & 1 spectraFigure 10 presents the plot of the correlation coefficient deviation, CCD[3], for 300-450 kHz frequency band. The CCD[3] damage metric tends to linearly decrease as the crack moves away from the sensor. Similar results were also obtained when the metric CCD[7] was used. The following conclusions can be drawn:

a) The crack presence significantly modifies the pointwise frequency response function, and hence the real part of the E/M impedance spectrum
b) This modification decreases as the distance between the sensor and the crack increases
c) The decrease tendency is not uniform for all frequency bands and this effect should be investigated further.

To obtain consistent results during the health monitoring process, the proper frequency band (usually in high kHz) and the appropriate damage metric must be used. Further work is needed on systematically investigating the most appropriate damage metric to be used for successful processing of the frequency spectra. The use of the α-th power of the correlation coefficient deviation, CCD$^\alpha$, $3 < \alpha < 7$, seems to give a good fit in the high frequency band 300-450 kHz.
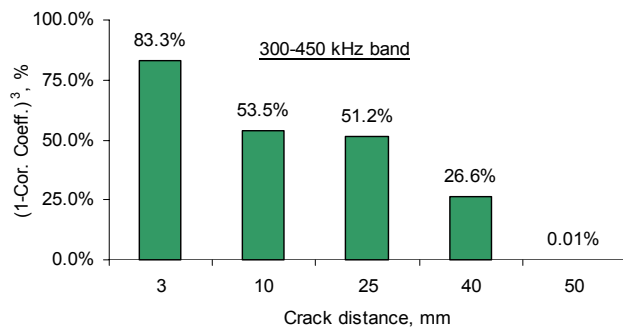
Figure 10. Variation of the correlation coefficient deviation (CCD) damage metric with the distance between the crack and the sensor in the 300—450 kHz band

CONCLUSIONS

In this paper, the application of E/M impedance method for damage detection in thin circular plates was discussed. The paper extends the quasi-static approach previously presented by Liang *et al.* (1994) and the one-dimensional dynamic approach presented by Giurgiutiu and Zagrai (2001b). A two-dimensional polar coordinates analysis for axis-symmetric vibrations is presented. The analytical solution incorporates and couples the dynamics of the structural substrate and the dynamics of the piezoelectric active sensor. The analytical model accounts for flexural and axial circular plate vibrations and predicts the E/M impedance response, as it would be measured at the piezoelectric active sensor's terminals during the health monitoring process. For the first time, the complete analytical solution for in-plane vibrations of piezoelectric disk with elastic constraint boundary conditions is derived. A set of experiments was conducted to support the theoretical investigation. Circular plate specimens were used to measure the electro-mechanical impedance spectra as predicted by the theory for a piezoelectric active sensor attached in the middle of the plate.

Seven flexural harmonics (0.7, 3, 7, 13, 20, 29 and 39 kHz) and one axial harmonic (37 kHz) of axis-symmetric vibrations were successfully identified by both theoretical predictions and experimental results. The experimental data also revealed other resonance peaks of residual amplitudes that can be attributed to non axis-symmetric modes that were inadvertently exited through small off-center deviations in sensor placement. Thus, we concluded that good matching of experimental and calculated E/M impedance signatures was obtained for both flexural and axial harmonics of the spectrum.

The sensor's sensitivity to the presence of structural damage was studied using five groups of plates, with the damage condition increasing gradually from pristine (Group 0) to severe damage (Group 4). The damage severity was controlled by gradually placing a simulated crack (EDM slit) closer and closed to the sensor. It was found that the crack presence dramatically modifies the E/M impedance spectrum, and that this modification increases as the distance between the sensor and the crack decreases. Consistent results were obtained especially at high frequencies (300-450 kHz). Several overall-statistics damage metrics were investigated: root mean square deviation (RMSD); mean absolute percentage deviation (MAPD); covariance change (CC); correlation coefficient deviation (CCD). We found that, in the 300-450 kHz band, the third power of the correlation coefficient deviation, CCD^3, correlated almost linearly with the damage location. Similar results were obtained with CCD^7.

The work reported in this paper has demonstrated the ability of permanently attached PZT active sensors to perform structural identification and damage assessment in thin circular plates through the E/M impedance method. Other important features of the work presented in this paper are:

a) The successful modeling of E/M impedance active sensor mounted on 2-D structure (circular plate) and verification of theoretical prediction through experimental results

b) The illustration of how the presence of a crack, located at various distances from the active sensor, modifies the broad-band E/M impedance spectrum recorded by the piezoelectric active sensor.

c) The observation that, among various overall-statistics damage metrics, the α-th power of the correlation coefficient deviation, CCD^α, $3 < \alpha < 7$, in the high frequency band 300-450 kHz., seemed to be the most successful in correlating with the distance between sensor and damage location.

A special novel feature of the present paper is the modeling of a piezoelectric active senor (PZT disk) vibration under elastic boundary conditions and the prediction of its broad band E/M impedance when installed on a circular plate.

ACKNOWLEDGMENTS

REFERENCES

Airey, J. (1911) "The Vibration of Circular Plates and their Relation to Bessel Functions", *Proc. Phys. Soc*., London, Vol. 23, 1911, pp.225-232

Ayres, T., Chaudhry Z., and Rogers C. (1996) "Localized Health Monitoring of Civil Infrastructure via Piezoelectric Actuator/Sensor Patches," *Proceedings, SPIE's 1996 Symposium on Smart Structures and Integrated systems, SPIE* Vol. 2719, pp. 123-131.

Chaudhry, Z., Sun, F. P, and Rogers C. A. (1994) "Health Monitoring of Space Structures Using Impedance Measurements," *Fifth International Conference on Adaptive Structures, Sendai, Japan,* 5-7 December, 1994; pp. 584-591.

Chaudhry, Z., Joseph, T., Sun, F., and Rogers, C. (1995) "Local-Area Health Monitoring of Aircraft via Piezoelectric Actuator/Sensor Patches," *Proceedings, SPIE North American Conference on Smart Structures and Materials, San Diego, CA*, 26 Feb. - 3 March, 1995; Vol. 2443, pp. 268-276.

Childs, B.; Lalande, F.; Chaudhry, Z.; Rogers, C. A. (1996) "High-Frequency Impedance Analysis for NDE of Complex Precision Parts," *Proceedings of the SPIE's 1996 Symposium on Smart Structures and Integrated Systems,* San Diego, CA, 25-29 February, 1996; SPIE Vol. 2717, pp. 237-243

Colwell, R.C. (1936) "The Vacuum Tube Oscillator for Membranes and Plates", *Journal of Acoustical Society of America*, Vol. 7, 1936, pp.228-230

Esteban, J.; Chaudhry, Z.; Lalande, F.; Rogers, C. A. (1996) "Theoretical Modeling of Wave Propagation and Energy Dissipation in Joints," *Proceedings, 37th AIAA/ASME/ASCE/AHS/ASC Structures, Structural Dynamics, and Materials Conference*, Salt Lake City, UT,

15-17 April, 1996

Giurgiutiu, V.; Zagrai, A. N. (2000) "Damage Detection in Simulated Aging-aircraft Panels Using the Electro-mechanical Impedance Technique", *Adaptive Structures and Material Systems Symposium, ASME Winter Annual Meeting*, Nov. 5-10, 2000, Orlando, Florida

Giurgiutiu, V., Reynolds, A., Rogers, C. A. (2000), "Experimental Investigation of E/M Impedance Health Monitoring of Spot-Welded Structural Joints" submitted for publication to the *Journal of Intelligent Material Systems and Structures*, v. 10, n. 10, October, pp. 802-812.

Giurgiutiu, V., Zagrai, A.N. (2001a) "Characterization of Piezoelectric Wafer Active Sensors", *Journal of Intelligent Material Systems and Structures*, Vol.11, p. 959-976, December 2000

Giurgiutiu, V., Zagrai, A.N. (2001b) "Embedded Self-Sensing Piezoelectric Active Sensors for On-Line Structural Identification", Submitted to: *Transactions of ASME, Journal of Vibration and Acoustics*, January 2001.

Giurgiutiu, V., Zagrai, A.N., Bao, J. (2001) "Embedded Active Sensors for In-situ Structural Health Monitoring of Aging Aircraft Structures", *Proceedings of the 7th ASME NDE Topical Conference*, NDE-Vol. 20, ASME 2001

IEEE Std. 176 (1987) *IEEE Standard on Piezoelectricity*, The Institute of Electrical and Electronics Engineers, Inc., 1987

Itao, K., Crandall, S.H. (1979) "Natural Modes and Natural Frequencies of Uniform, Circular, Free-Edge Plates", *Journal of Applied Mechanics*, Vol. 46, 1979, pp. 448-453

Kunukkasseril, V.X., Swamidas, A.S.J. (1974) "Vibration of Continuous Circular Plates", *International Journal of Solids Structures*, Vol. 10, 1974, pp. 603-619

Liang, C., Sun, F. P., and Rogers C. A. (1994) "Coupled Electro-Mechanical Analysis of Adaptive Material System-Determination of the Actuator Power Consumption and System energy Transfer", *Journal of Intelligent Material Systems and Structures*, Vol. 5, January 1994, pp. 12-20

Liessa, A. (1969) "Vibration of Plates", Published for the Acoustical Society of America through the American Institute of Physics, Reprinted in 1993

Lopes, V.; Park, G.; Cudney, H.; Inman, D. J. (2000) "A Structural Health Monitoring Technique Using Artificial Neural Network and Structural Impedance Sensors," *Journal of Intelligent Material Systems and Structures*, Vol. 11, No. 3, pp. 206-214

Monaco, E., Franco, F., Lecce, L. (2001) "Experimental and Numerical Activities on Damage Detection Using Magnetostrictive Actuators and Statistical Analysis", *Journal of Intelligent Material Systems and Structures*, Vol. 11, No. 7, July 2000, pp. 567-578

Onoe, M., Jumonji, H. (1967) "Useful formulas for piezoelectric ceramic resonators and their application to Measurement of parameters", *IRE*, Number 4, Part 2, 1967

Park, G.; Cudney, H.; Inman, D. J. (2000a) "An Integrated Health Monitoring Technique Using Structural Impedance Sensors," *Journal of Intelligent Material Systems and Structures*, Vol. 11, No. 6, pp. 448-455

Park, G.; Cudney, H.; Inman, D. J. (2000b) "Impedance-based Health Monitoring of Civil Structural Components", *ASCE Journal of Infrastructure Systems*, Vol. 6, No. 4, pp. 153-160

Park, G.; Cudney, H.; Inman, D. J. (2001) "Feasibility of Using Impedance-based Damage Assessment for Pipeline Systems", *Earthquake Engineering & Structural Dynamics Journal*, Vol. 30, No. 10, pp. 1463-1474

Pugachev, S. I, Ganapol'sky, V. V., Kasatkin, B. A., Legusha, F. F., Prud'ko, N. I. (1984) Handbook "Piezoceramic

Transducers", *Sudostroenie*, St.- Petersburg (In Russian)

Rao, J.S. (1999) "Dynamics of Plates". Marcel Dekker, Inc., Narosa Publishing House, 1999

Soedel, W. (1993) "Vibrations of Plates and Shells", Marcel Dekker, Inc., 1993

Sun, F. P., Liang C., and Rogers, C. A. (1994) "Experimental Modal Testing Using Piezoceramic Patches as Collocated Sensors-Actuators", *Proceeding of the 1994 SEM Spring Conference & Exhibits*, Baltimore, MI, June 6-8, 1994.

Sun, F. P., Chaudhry Z., Rogers C. A., Majmundar M. (1995) "Automated Real-Time Structure Health Monitoring via Signature Pattern Recognition," *Proceedings, SPIE North American Conference on Smart Structures and Materials,* San Diego, CA, 26 Feb. -3 March, 1995; Vol. 2443, pp. 236-247

Tseng, K. K.-H.; Bhalla, S.; Gupta, A. (2000) "Performance of Smart Piezoceramic Patches in Health Monitoring of a RC Bridge" *Smart Materials and Structures¸* Vol. 9, No. 4, August 2000, pp. 533-542

Tseng, K. K.-H.; Soh, C. K.; Naidu, A. S. K. (2001) "Non-Parametric Damage Detection and Characterization Using Smart Piezoceramic Material" *Smart Materials and Structures* (in press)

Wah, T. (1962) "Vibration of Circular Plates", *Journal of Acoustical Society of America*, Vol. 34, 1962, pp.275-281

Zagrai A. N., Giurgiutiu V. (2001) "Utilization of Electro Mechanical Impedance Method for Structural Identification of Circular Plates", REPORT # USC-ME-LAMSS-2001-104, November 7, 2001